AN INTERNATIONAL TURBULENCE COMPARISON EXPERIMENT (ITCE 1976)

A. J. DYER, J. R. GARRATT, R. J. FRANCEY, I. C. McILROY, N. E. BACON, P. HYSON

CSIRO Division of Atmospheric Physics, Aspendale Victoria, Australia

E. F. BRADLEY, O. T. DENMEAD

CSIRO Division of Environmental Mechanics, Canberra, Australia

L. R. TSVANG, Y. A. VOLKOV, B. M. KOPROV, L. G. ELAGINA

Institute of Atmospheric Physics, U.S.S.R. Academy of Science

K. SAHASHI, N. MONJI, T. HANAFUSA, and O. TSUKAMOTO

Okayama Univ., Univ. of Osaka, Met. Research Institute, Univ. of Kyoto, Japan

P. FRENZEN, B. B. HICKS*, M. WESELY

Argonne National Laboratory, Illinois, U.S.A.

M. MIYAKE

Univ. of British Columbia, Canada

W. SHAW

Univ. of Washington, Seattle, U.S.A.

(Received 14 July, 1982)

Abstract. Turbulence data for the International Turbulence Comparison Experiment (ITCE) held at Conargo, N.S.W. (35°18′ S., 145°10′ E.) during October, 1976 are analysed.

The standard deviation $(\overline{s'^2})^{1/2}$ and covariance $\overline{w's'}$ measured by a number of instruments and instrument arrays have been compared to assess their field performance and calibration accuracy. Satisfactory agreement, i.e. typically 5% for $(\overline{s'^2})^{1/2}$ (except in humidity) and of the order of 20% for $\overline{w's'}$, was achieved, but only after consideration of:

(1) Instrumental response at high frequencies.
(2) Flow distortion induced by instruments and supporting structures.
(3) Spatial separation of instruments used for covariance measurements.
(4) Statistical errors associated with single point measurements over a finite averaging time, and with lateral separation of two sensor arrays being compared.

1. Historical Background

In the last two decades a considerable amount of instrument development has taken place for the measurement of turbulence in the lower atmosphere, and numerous publications of observational material have appeared. However, considerable discrepancies have occurred in the literature, and the possibility that differences in the various techniques being employed could contribute to these prompted a number of informal comparisons of instrument performance. These took place in the U.S.A. in 1965

* Present Affiliation Atmospheric Turbulence and Diffusion Laboratory NOAA, Oak Ridge, Tennessee.

Boundary-Layer Meteorology **24** (1982) 181–209. 0006–8314/82/0242–0181$04.35.

(Businger *et al.*, 1969), in Australia in 1966 (Businger *et al.*, 1967), and in Canada in 1968 (Miyake *et al.*, 1971). These comparisons yielded much information of value, but pointed also to the need for further improvements and comparisons.

The first major international comparison was organised by the Institute of Atmospheric Physics of the U.S.S.R. in 1970 (Tsvang *et al.*, 1973). Groups from Russia, Canada, U.S.A. and Australia participated at Tsimlyansk. The performance of the various sensors was carefully assessed by spectral analysis, and one of the major conclusions was that 'Periodic verifications of instruments for the measurement of turbulent characteristics seem to be both necessary and productive. In each such comparison which has been reported, unexpected deficiencies have been revealed. Such a comparison is particularly advisable in conjunction with such wide-ranging efforts for GARP.'

The Tsimlyansk experiment in 1970 was essentially a comparison of velocity and temperature sensors, and international dialogue since 1970 called for a consolidation of these comparisons, together with an extension to fast-response humidity sensors. At the same time it was hoped that a data set could be assembled which would provide definitive information on, for example, flux-profile relationships, the von Karman constant and the Kolmogarov constants.

With this in mind the CSIRO Division of Atmospheric Physics proposed to host a second major International Turbulence Comparison Experiment (ITCE) during October, 1976, and accordingly invited international groups to participate. Scientists from Russia, Japan, U.S.A., Canada and Australia took part, with an observer from France. This comparison of turbulence instruments is referred to generally as the Central-Core Experiment. Other groups from CSIRO and some Australian universities also took part in a series of peripheral experiments relevant to their fields of special interest.

The CSIRO Division of Atmospheric Physics provided background micrometeorological measurements, including net radiation and ground heat flux, wind direction, wind speed, temperature and humidity profiles up to 16 m height, a complete set of eddy-flux covariance measurements at two heights, and a lysimetric determination of the evaporative flux. The CSIRO Division of Environmental Mechanics obtained shearing stress measurements with two drag plates, two sets of eddy flux covariance measurements based on sonic anemometers, and wind profiles from 0.25 to 8 m height. This part of the experiment is referred to generally as the Micro-Meteorological Support Experiment. The complete data sets both for the central core experiment and the micrometeorological support experiment are reported elsewhere (Garratt *et al.*, 1979; Dyer *et al.*, 1981).

2. Site Planning and Layout

A preliminary survey of possible sites in northern Victoria, and southern New South Wales, was carried out during late 1975 and early 1976, and a site was selected some 15 km NNW of Conargo, near Deniliquin, N.S.W. (see Figure 1) in open grazing country on the 'Boonoke' Station. During the months prior to October 1976, the area was gradually established as an observational site.

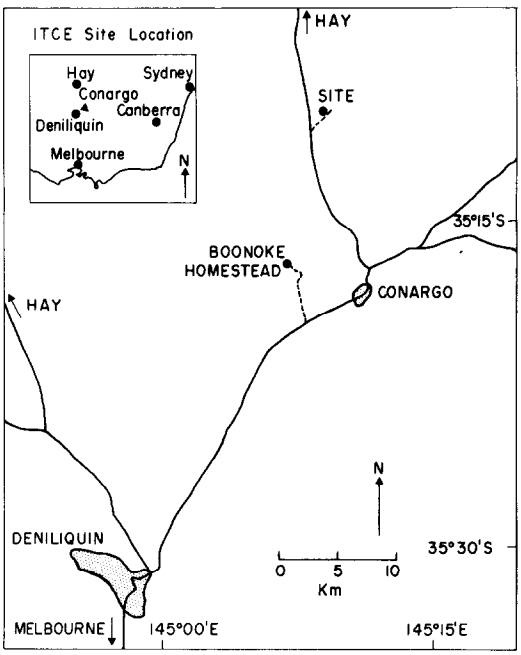

Fig. 1. Geographical location of ITCE site.

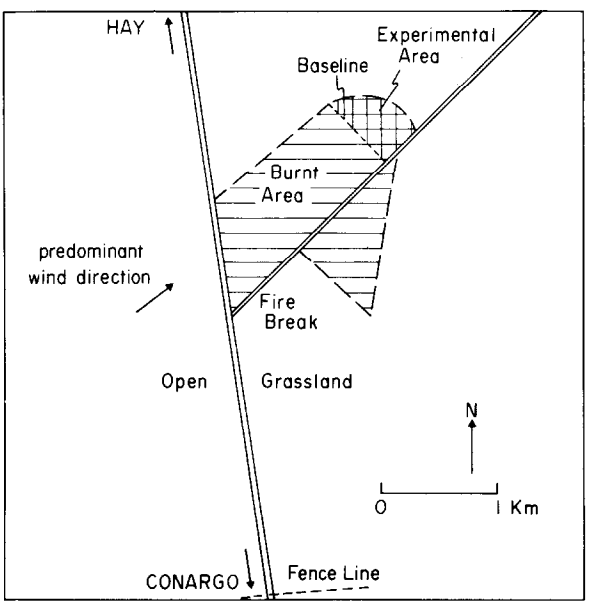

Fig. 2. Immediate vicinity of experimental area showing instrument lower baseline and outline of burnt grass.

In the last week of preparation a grass fire occurred on the site due to a diesel generator malfunction, causing some concern about the adequacy of the fetch. A number of controlled burns were immediately carried out to extend the range of uniform blackened earth out to a distance of about 1–1.5 km. The precise details of the burnt area are shown in Figure 2. During the course of the experimental period some moderate falls of rain occurred, so that the area gradually changed from blackened earth to a sparse covering of short blades of green grass. The area outside the burnt patch supported a moderate cover of salt-bush and native grasses with an average height of about 0.5 m.

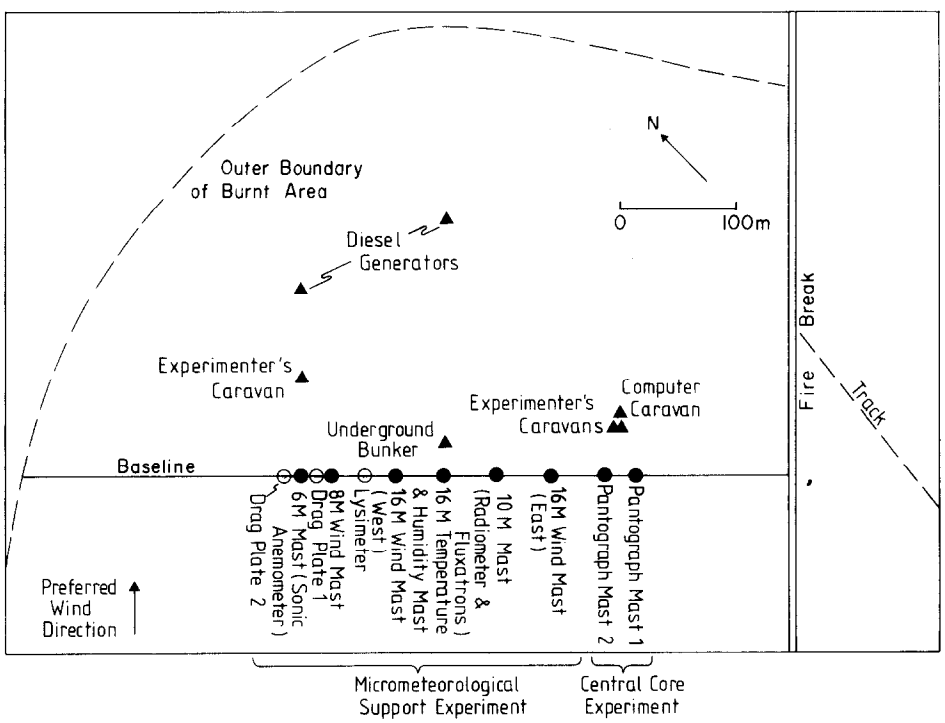

Fig. 3. Layout of experimental area showing baseline, firebreak, northern boundary of burnt grass area, and location of main instruments or structures.

The layout of the experimental site is illustrated in Figure 3, and a general view shown in Figure 4. The central core sensors were mounted on two pantograph masts (Figure 5) designed and constructed similarly to an earlier Russian model (Tsvang *et al.*, 1973). These pantograph masts were 25 m apart, with the experimenters' caravans located 40 m to the rear. From the experimenters' caravans, the signal lines travelled a further 15 m to the computer caravan. The nominal height of the horizontal mounting bars of the pantograph masts was 4 m when fully raised.

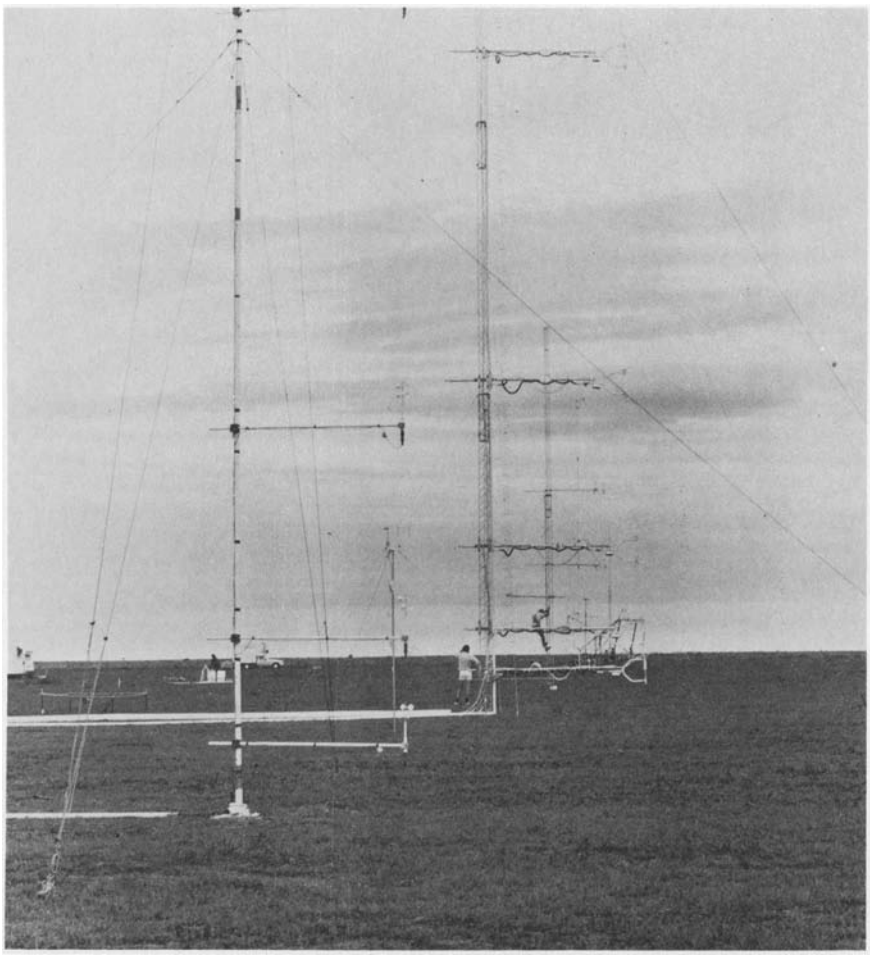

Fig. 4. View of the site looking along the line of profile-measuring masts.

3. Details of Sensors

The following is a brief summary of the sensors used in the experiment. Fuller descriptions are available in Garratt *et al.* (1979) and Dyer *et al.* (1981).

3.1. Central core experiment

Each sensor is supplied with a code, the first letter indicates the group (i.e., R = Russian, I = Illinois, etc.), the second and third letters identify the sensor (i.e., JT = Japanese thermometer, CTW = Canadian wet bulb, etc.).

(i) Russia

RU, RV, RW	Sonic anemometers in three dimensions.
RT	Resistance thermometer (5.6 μm tungsten).
RQ	Infra-red hygrometer (0.15 m gap with return mirror).

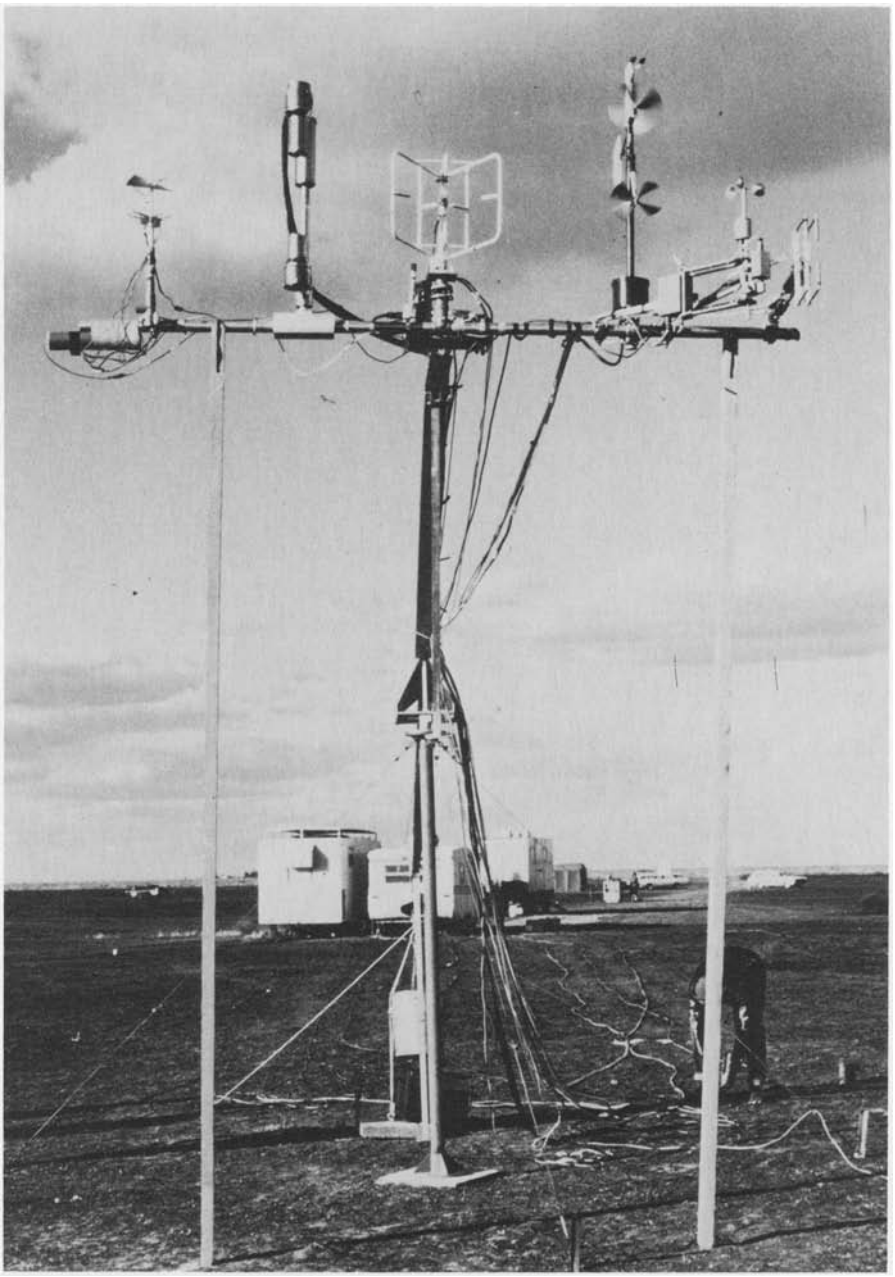

Fig. 5. View of one of the two pantograph masts with central core sensors mounted.

(ii) Illinois

IW	Vertical Gill propeller anemometers.
IU	Low-inertia, 6 cup anemometer.
ITB	Thermistor thermometer (125 μm diam).

ITF	Resistance thermometer (2–3 μm diam).
IQ	Lyman-α hygrometer (10 mm gap).

(iii) Canada

CU, CW	Two Gill propeller anemometers, one horizontal (CU), the other 57.5 degrees to horizontal.
CQ	Thermocouple psychrometer, incorporating CT, CTW (25 μm diam thermocouples).

(iv) Japan

JU, JV, JW, JUV	Three-dimensional sonic anemometers, with total wind vector.
JQT	Thermocouple psychrometer incorporating JT, JTW (120 μm diam thermocouples).
JQA	Analog circuit thermocouple psychrometer (100 μm diam).

(v) Washington

WW	1-dimensional sonic anemometer.
WU	Low-inertia cup anemometer.
WT	Thermocouple thermometer (25 μm diam).
WQ	Lyman-α hygrometer (5 mm gap).

(vi) Australia

AW	Vertical Gill propeller.
AU	Low-inertia 6-cup anemometer.
AT	Thermistor thermometer (response time 0.1–0.2 s).
AQ	Infra-red hygrometer (gap 0.2 m).

3.2. Micrometeorological support experiment

(i) Wind profiles – Low-inertia 6-cup anemometers, mounted at heights of 1.00, 2.00, 4.00, 8.00, and 16.00 m on 2 masts.

(ii) Wind profile – Low-inertia cup anemometers mounted at heights of 0.25, 0.50, 0.71, 1.00, 1.41, 2.00, 2.83, 5.56, and 8.00 m.

(iii) Temperature profile – Quartz-crystal thermometers mounted in aspirated radiation shields at 1.08, 1.97, 3.97, 8.00, and 16.00 m height. Sampled once a minute, with absolute accuracy ± 0.1 °C, relative accuracy ± 0.01 °C.

(iv) Specific humidity profiles – Air was drawn from the various levels through heated plastic tubing. All air streams were first brought to a common temperature by passing through 6 m long coils of copper tubing immersed in a large stirred water bath. Subsequently, wet- and dry-bulb thermometers, using quartz-crystal thermometers determined the specific humidity at levels of 1.08, 1.97, 3.97, 8.00, and 16.00 m height. The relative accuracy was ± 0.025 g kg^{-1}. Additional profile measurements were also taken by an infra-red hygrometer and an infra-red gas analyser.

(v) Evaporation (Lysimeter) – Evaporation was measured directly using a 10-tonne monolith lysimeter, 2 × 1.5 m in surface area, 1.5 m depth, based on an earlier design (McIlroy, 1973 – see Garratt *et al.*, 1979).

(vi) Surface Stress (Drag Plates) – Two identical 1.83 diam drag plates (Lynch and Bradley, 1974) recorded the surface stress. Twice during the course of the experiment, the surfaces were remodelled to match the changing appearance of the surrounding area.

(vii) Eddy fluxes – 'Fluxatrons' were operated at heights of 5.5 and 8.5 m. Each comprised a Gill propeller anemometer for vertical windspeed, a light-weight 6-cup anemometer for horizontal wind speed, a fine glass-bead thermistor for temperature, and an infra-red hygrometer for specific humidity (Hyson and Hicks, 1975). The resulting fluxes were corrected for high-frequency loss and instrument tilt. In addition, two 3-component sonic anemometers were operated at heights of 3.2 and 5 m, each incorporating a fast-response platinum wire thermometer. The lower sensor array also employed an infra-red hygrometer similar to those used with the 'Fluxatrons'.

(viii) Net Radiation and Ground Heat Flux – Net radiation was determined with a standard commercial polythene-shielded net radiometer with an accuracy of $\pm 5\%$. Five commercial ground heat-flux plates (Middleton) were positioned at a depth of 10 mm below the surface and connected in series. The absolute accuracy of the flux-plates was $\pm 15\%$, but allowance must also be made for heat storage in the soil layer above the plates.

4. Data Acquisition and Processing

4.1. Central Core Acquisition

The computer caravan housed two Hewlett-Packard computers. A HP2100 was dedicated to central core data acquisition, with some assistance from a HP21MX (which also processed the micrometeorological support data). Each channel was sampled at 33.3 Hz, and the digitized data recorded on magnetic tape. A routine central core run lasted 32.77 min corresponding to the acquisition of 2^{16} voltage samples on each of 32 channels.

4.2. Micrometeorological Support Acquisition

Within the underground bunker the various quartz crystal thermometers were connected, in turn, through a co-axial scanner to a Hewlett-Packard Model 2910A Quartz Thermometer Unit. A Solartron Data Transfer unit controlled the sequence and transferred data to a paper tape punch and the central core computer HP21MX. Voltage outputs from the thermometers, the psychrometer water bath thermometer, net radiometer, heat flux plates, wind vane, infra-red hygrometer and infra-red gas analyser, were each scanned by the Data Transfer Unit at the rate of one per minute.

4.3. Central Core Processing

The central core data, having been recorded digitally on magnetic tape in the field, were subsequently spectrally analysed using a fast-Fourier Transform using the CSIRO central computer (CDC Cyber 76). The spectral estimates obtained were averaged

in bands with the central frequencies differing by a factor of $\sqrt{2}$, and extended in frequency from 0.0005 to 16.666 Hz. Spectral estimates corresponding to frequencies higher than 8.33 Hz were not included in the final print-out in order to minimise aliasing effects. In addition, the spectral estimates at the lowest frequency (0.0005 Hz) were omitted because of lack of statistical confidence.

As a check on the computations, all variances were calculated directly from the raw data and compared with integrated spectral estimates. Accurate agreement was obtained in all cases. In a few instances this procedure was performed also for covariances and co-spectra. A further check was made by spectral analysis of a sine function recorded on some runs. These analyses gave correct values for amplitude and frequency.

5. Instrumental and Statistical Limitations

For preliminary analysis the spectral data were combined to provide variances and covariances in three frequency bands covering a frequency range constrained by t_R, the duration of each run, and the sampling frequency of 33.3 Hz. The choice of band-widths was made by reference to published spectra (Kaimal *et al.*, 1972) to give three spectral slices; slice A with $n < 0.005$ Hz, slice B with $0.005 < n < 0.195$ Hz and slice C with $n > 0.195$ Hz. Slice B is intended to provide variance data capable of providing a meaningful comparison of calibration factors, in that it should be essentially unaffected by either lack of high frequency response in any particular sensor or low frequency drift of instrumental or atmospheric origin.

An important aspect of the experiment is to assess the agreement that can be expected between two physically-separated instruments or instrument arrays measuring the variance or covariance at the same time. In the following this is done by reference to published spectra, time/space correlations and other experimental evidence (Kaimal *et al.*, 1972; Lumley and Panofsky, 1964; Pasquill, 1962; Koprov and Sokolov, 1973). Figure 6, for example, using data from these papers provides information on the correlation coefficients (r_x, r_y) between the various sensors as a function of separation in the x and y direction, where, for the x-direction, (i.e., mean wind direction), autocorrelations have been converted to space correlations by means of $x = \bar{u}t$. Also indicated on Figure 6 are the integral length scales L_x and L_y for the various situations. Note that in general $L_y \ll L_x$.

Let us first assess the probable error in a variance or covariance measured by a single instrument or sensor array.

Each sensor or sensor array measures a quantity f (e.g., u'^2, T'^2, $u'w'$, etc.) in a time series of duration t_R, giving a local mean value $\bar{f}$. It is presumed that the value required is the ensemble average $\hat{f}$ (i.e., as measured by a large number of perfect instruments at the same time). For $\bar{f}$ to converge on $\hat{f}$ requires a choice of t_R such that

$$t_R \gg t_x .$$

Here t_x is the integral scale of the autocorrelation function related approximately to the

peak frequency, n_{max}, of the spectrum $n\phi(n)$, by

$$t_x = (2\pi n_{max})^{-1} .$$

The choice of t_R = 32 min is consistent, for a measurement height of 4 m, with observed values of n_{max} for velocity, temperature and humidity spectra as given by Kaimal *et al.* (1972).

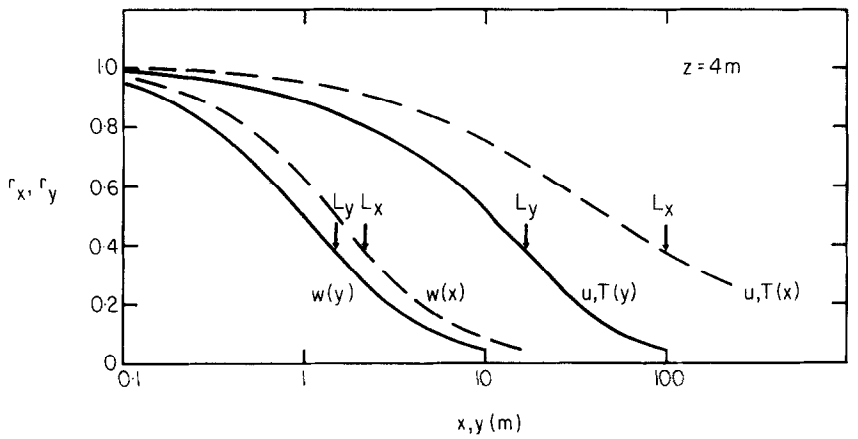

Fig. 6. Autocorrelation functions for the longitudinal (x, in the mean wind direction) and transverse (y) directions. L_x, L_y are the implied integral space values for u, w, and T at a height of 4 m and wind speed 5 m s^{-1}.

For any point measurement of f, the probable relative error (ε) in determining $\hat{f}$ from a finite time series is given by Lumley and Panofsky (1964) as

$$\varepsilon^2 = \frac{2t_x}{t_R} \frac{\overline{(f-\hat{f})^2}}{\hat{f}^2} .$$

For the variance of a Gaussian distribution, approximately so for the atmospheric case, we have, according to Lumley and Panofsky (1964),

$$\frac{\overline{(f-\hat{f})^2}}{\hat{f}^2} = 2 .$$

Thus, ε_v, the probable relative error in a variance, will be given by

$$\varepsilon_v^2 = 4t_x/t_R .$$

For a covariance, the probable relative error ε_c will be given (Wyngaard, 1973) by

$$\varepsilon_c^2 = \frac{2t_x}{t_R} (1 + r_{ij}^{-2})$$

where r_{ij} is the cross-correlation between two variables i, j at a single point.

The corresponding equation for a spectral band is obtained by substituting $(2\pi n_c)^{-1}$ for t_x. We thus have

$$\varepsilon_v^2(\text{BAND}) = 4(2\pi n_c)^{-1}/t_R\,,$$

where n_c is the central frequency of the band. Since we are only attempting to assess the order of magnitude of the probable errors, a precise definition of n_c is unnecessary.

Turning now to the possible differences between the two arrays separated laterally by varying distances (y) of 1 to 125 m, we have variances or covariances $\overline{f_A}$ and $\overline{f_B}$ for sensor arrays A and B separated by a distance y and measured for each of p runs.

The observed normalised r.m.s. difference δ_{obs} is then defined as

$$\delta_{\text{obs}}^2 = [\{(\overline{f_A} - [\overline{f_A}]) - (\overline{f_B} - [\overline{f_B}])\}^2]/[\overline{f_B}]^2$$

where allowance is made for differences in the p run means, e.g., arising from small sensor gain differences. Here $[\ ] = p^{-1}\Sigma_p$. For large enough y, the contribution of statistical errors will be

$$\delta^2 = \varepsilon_{f_A}^2 + \varepsilon_{f_B}^2 = 2\varepsilon^2,$$

where ε can be either ε_v or ε_c.

It seems reasonable to assume that at intermediate values of y, the dependence of δ^2 will be of the general form

$$\delta^2 = 2\varepsilon^2 F(y/L_y)\,.$$

If y is sufficiently small ($y \ll L_y$) so that $r_y \to 1$ (assuming perfect sensors), we would expect $\delta \to 0$, inasmuch as array separation and sensor separation raise similar problems.

Here we adopt a simple linear form $F(y/L_y) = 1 - r_y$, so that we write

$$\delta^2 = 2\varepsilon^2(1 - r_y)\,.$$

With these considerations, especially the published spectra of Kaimal *et al.* (1972), we are led to the following values at a height of 4 m.

For w	$n_{max} \approx 0.5$ *Hz*,	$t_x \approx 0.3$ s,	$L_x \approx$ 2 m
For *u, T, q*	$n_{\max} \approx 0.01$ Hz,	$t_x \approx 16$ s,	$L_x \approx 100$ m
For *uw, wT, wq*,	$n_{\max} \approx 0.1$ Hz,	$t_x \approx 1.6$ s,	$L_x \approx$ 10 *m*

And for slice B, $n_c \approx 0.03$ *Hz*.

Hence we find an assessment of the probable error in one sensor and the r.m.s. difference between two sensors (or arrays) as a function of lateral distance y as listed in Table I. For the covariance calculations, appropriate values of r_{ij} are taken from Kaimal *et al.* (1972) for the mean z/L encountered. For the comparison to be presented, lateral y's are of the order 1 and 25 m, and for the covariances 125 m (whence $r_y = 0$).

In covariance measurements, spatial separation of the sensors, or the physical dimensions of the sensor, will cause a distortion of the true covariance. The effect is particularly severe for lateral separations since $L_y \ll L_x$. Defining ζ as the ratio of measured to true covariance, the data of Koprov and Sokolov (1973) suggest the following values of ζ (Table II) for a range of lateral separation relevant to the subsequent discussion.

TABLE I

Statistical limitations in sensor comparison

Quantity	Probable error in one sensor (%)	r.m.s. difference (%) between two sensors (or arrays)		
		y = 1 m	25 m	125 m (or ∞)
Total w variance	2.6	2.6	3.7	3.7
Total u, T, q variance	18	8.5	22	26
Slice B, w variance	11	8	14	14
Slice B, u, T, q variance	11	4	11	14
uw covariance	16	–	–	23
wT, wq covariance	10	–	–	14

TABLE II

Values of ζ, the ratio of measured to true covariance, as a function of separation y

	y = 0.1 m	0.2 m	0.5 m
uw covariance	0.9	0.8	0.6
wT and wq covariances	0.95	0.9	0.8

6. Flow Distortion

Distortion of the flow by the sensors themselves and the supporting structures is a matter of concern in all turbulence measurements. Measurements of the momentum covariances are well known to be particularly vulnerable in this area. Dyer (1981) has attempted to analyse the distortion introduced by the horizontal support cylinder, and concluded that this was very small and that there was a strong similarity to the correction by the normal tilt equations. Hence the flow distortion corrections applied in the present analysis have followed the conventional tilt equations which for momentum is of the form:

$$\overline{u'w'} = \overline{u'_m w'_m} \cos 2\theta + \tfrac{1}{2} \sin 2\theta (\overline{u'^2} - \overline{w'^2}),$$

where the subscript m indicates a measured quantity and θ is the (equivalent) angle of tilt.

Wyngaard has questioned the adequacy of this approach (Wyngaard, 1982) and an inspection of Wyngaard's more elaborate theory suggests that a corresponding correction equation would be similar to the above Equation but with the $(\overline{u'^2} - \overline{w'^2})$ term replaced by $(\overline{u'^2} + \overline{w'^2})$ (Dyer, 1982). For typical values of the parameters, this would correspond to a correction of the order of 20% per degree rather than the 14% implied by the tilt equation. At small distances from the horizontal support arm, the correction would be even larger. These considerations should be borne in mind in relation to the comparisons to be presented in a later section.

However, it seems abundantly clear that in some cases the sensors themselves would have introduced significant distortion of the flow to an extent that may not be readily predictable, and considerable care must be taken in the basic design of turbulence sensors.

7. Results and Preliminary Conclusions

In this section we shall provide an assessment of the relative performance of sensors. Some of the reference data used are provided in a CSIRO Technical Report (Garratt *et al.*, 1979).

We examine sensor performance through consideration of the measured quantity $\sigma = (\text{variance})^{1/2}$ in the middle frequency band discussed earlier. We then proceed to a comparison of the measured covariances for the whole frequency range.

In the σ analysis, we have adopted the method of choosing one of the central core sensors as the reference sensor, with other sensors then compared with this reference. It is recognized that the reference itself may not be perfect, but selection is on the basis that

(i) the physics of that instrument is well understood;

(ii) there has been a long and satisfactory record of technical development;

(iii) the reference sensor has an adequate high frequency response;

(iv) there is a large data set available for the reference sensor for comparison purposes.

This technique is preferred to such alternatives as that of comparing with the mean of all sensors which (a) may be of uneven quality and (b) would demand the neglect of data when not all sensors were operating.

The reference sensors so chosen were: the Japanese sonic anemometer (vertical velocity JW, longitudinal horizontal velocity JU), the Russian temperature (RT) and humidity (RQ) sensors. Reference arrays used in the covariance analysis will be discussed later. The probable effects of flow distortion and sensor response in slice B of the variances have been assessed as small and so are ignored.

7.1. Comparison of σ in slice *B*

7.1.1. *w-sensors* (Reference JW): σ_w

The individual values of σ_w in slice *B* are plotted in Figure 7, and relevant information given in Table III. Note that here, as well as in the following tables, we estimate the errors in σ_w, σ_u, σ_q, σ_T and not in σ_w^2, σ_u^2, σ_q^2, σ_T^2 as in Table I.

Referring to δ, measured values are somewhat greater than those predicted, although some increases with separation are apparent. Highly significant differences from the reference sensor in the case of Δ are seen for IW, AW, and WW. These appear to be a reflection of calibration differences since, even for the mechanical anemometers, (CW, AW, IW) sensor response considerations suggest a negligible loss within slice *B*.

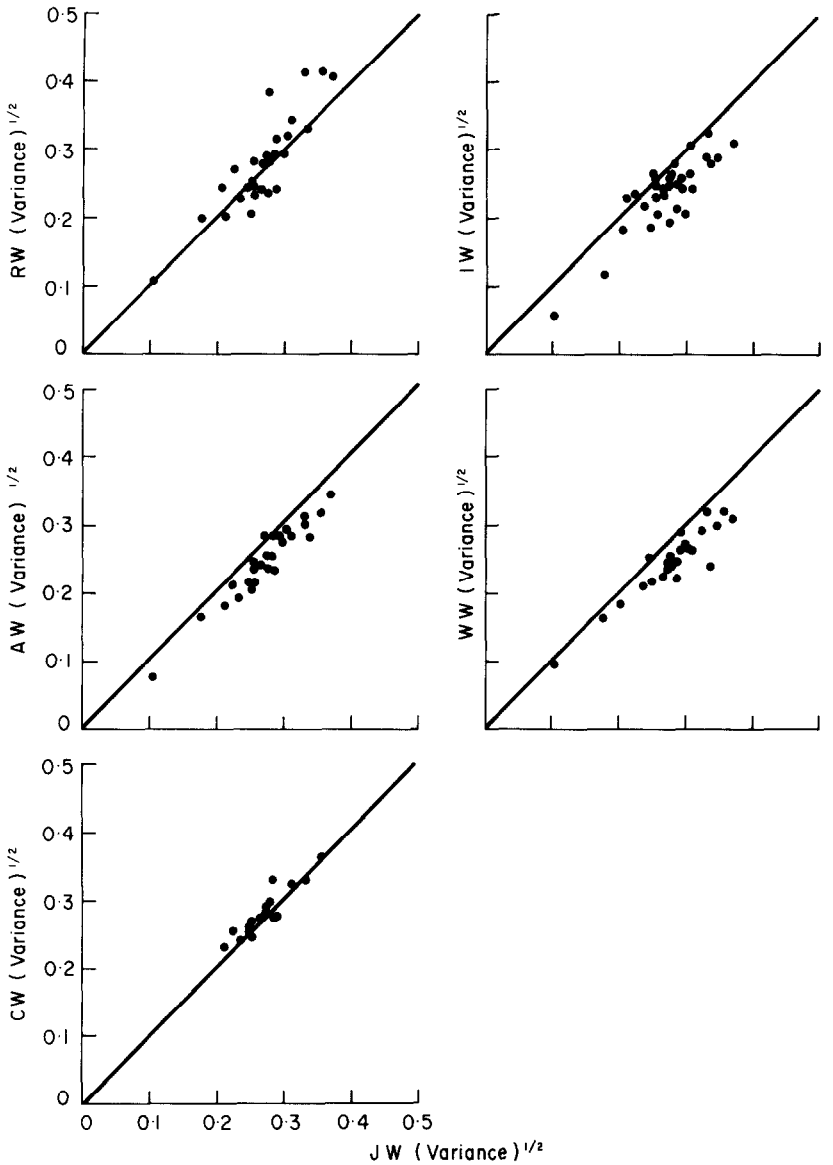

Fig. 7. Comparison of w-sensors in the form of σ_w in the middle spectrum band.

7.1.2. *u-sensors* (Reference JU): σ_u

The individual values of σ_u in slice B are plotted in Figure 8, and relevant information given in Table IV.

Table IV shows good calibration agreement, i.e., to within a few per cent in Δ. Measured values of δ are generally somewhat greater than those predicted.

TABLE III

Comparison of σ_w for w-sensors in slice B. The reference sensor JW shares a mast with CW, WW (separation $\simeq$ 1 m); sensors RW, IW, AW are on a second mast (separation from JW $\simeq$ 25 m)

Sensor	No. of runs	RMS difference δ (%)	Predicted RMS difference δ (%)	Mean difference Δ (%)
CW	18	5.5	4	3.3
WW	25	7.5	4	−12.5
RW	29	13.0	7	4.8
IW	32	10.3	7	−12.4
AW	16	5.9	7	−9.5

TABLE IV

Comparison of σ_u for u-sensors in slice B with reference sensor JU. Other details as in Table III

Sensor	No. of runs	RMS difference δ (%)	Predicted RMS difference δ (%)	Mean difference Δ (%)
CU	18	5.0	2	5.6
WU	27	5.4	2	5.8
RU	24	6.5	5.5	0.9
IU	32	7.0	5.5	1.7
AU	31	8.3	5.5	3.4

TABLE V

Comparison of σ_T for sensors in slice B. The reference sensor RT shares a mast with ITB, AT (separation $\simeq$ 1 m). Sensors CT, JT, WT are on a second mast (separation from RT $\simeq$ 25 m)

Sensor	No. of runs	RMS difference δ (%)	Predicted RMS difference δ (%)	Mean difference Δ (%)
ITB	25	13.0	2	−1.0
AT	32	3.7	2	−0.2
CT	23	9.3	5.5	−6.5
JT	32	7.9	5.5	−9.0
WT	21	7.6	5.5	−4.9

7.1.3. *T-sensors* (Reference RT): σ_T

The individual values of σ_T in slice B are plotted in Figure 9, and relevant information given in Table V.

Again, measured values of δ are somewhat larger than predicted with that for ITB appearing somewhat anomalous. Several sensors show considerable values of Δ suggesting calibration differences.

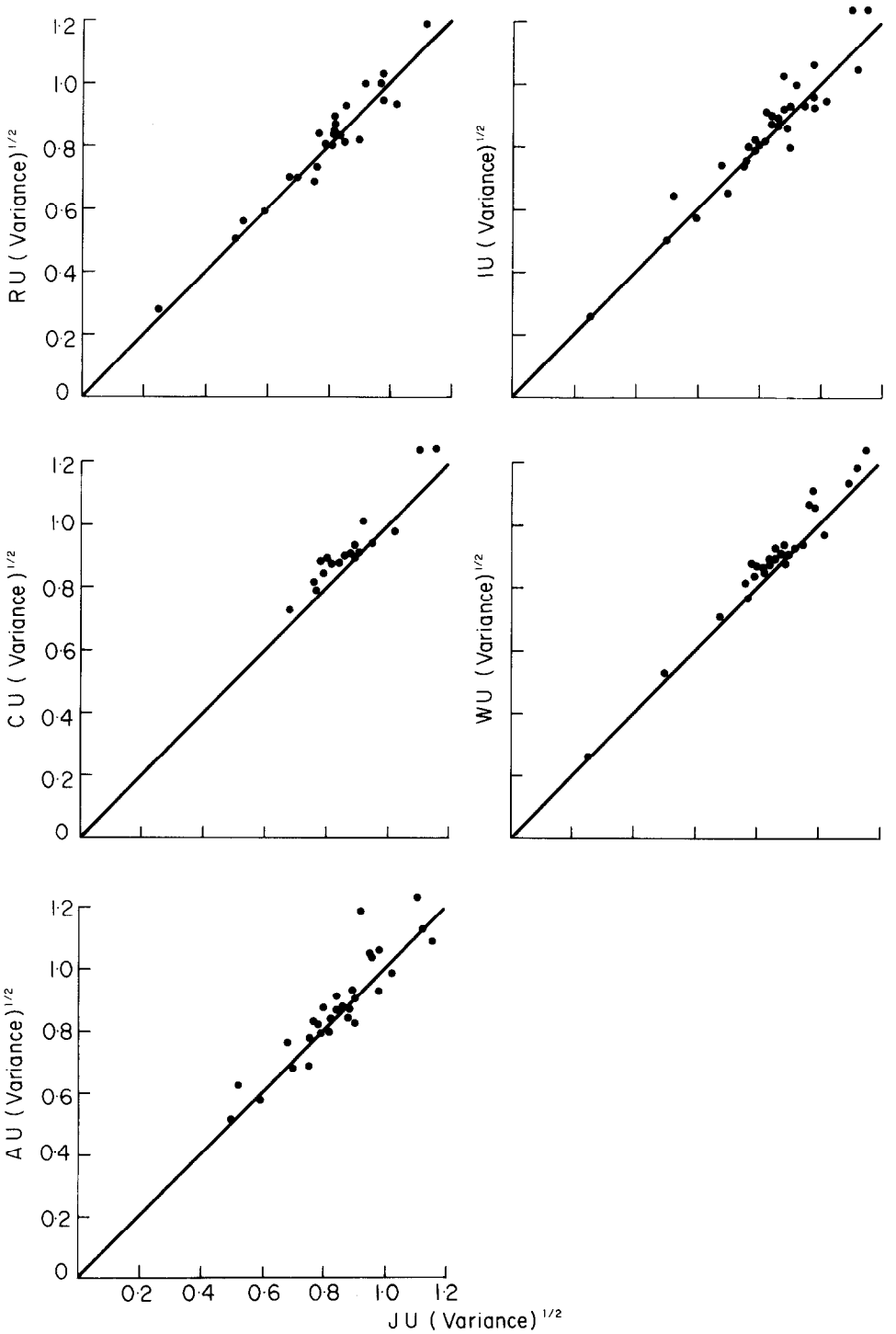

Fig. 8. Comparison of u-sensors in the form of σ_u in the middle spectrum band.

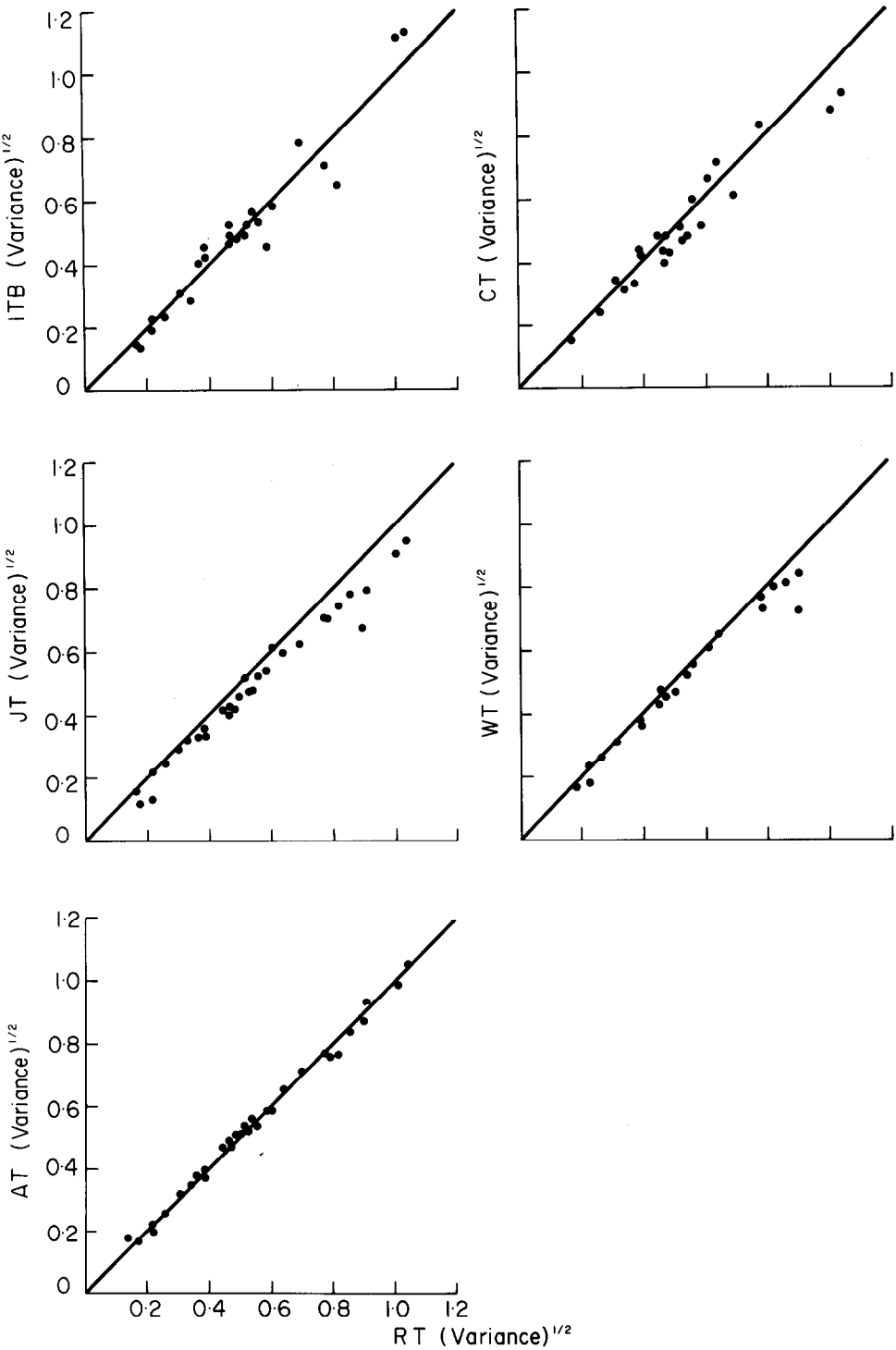

Fig. 9. Comparison of T-sensors in the form of σ_T in the middle spectrum band.

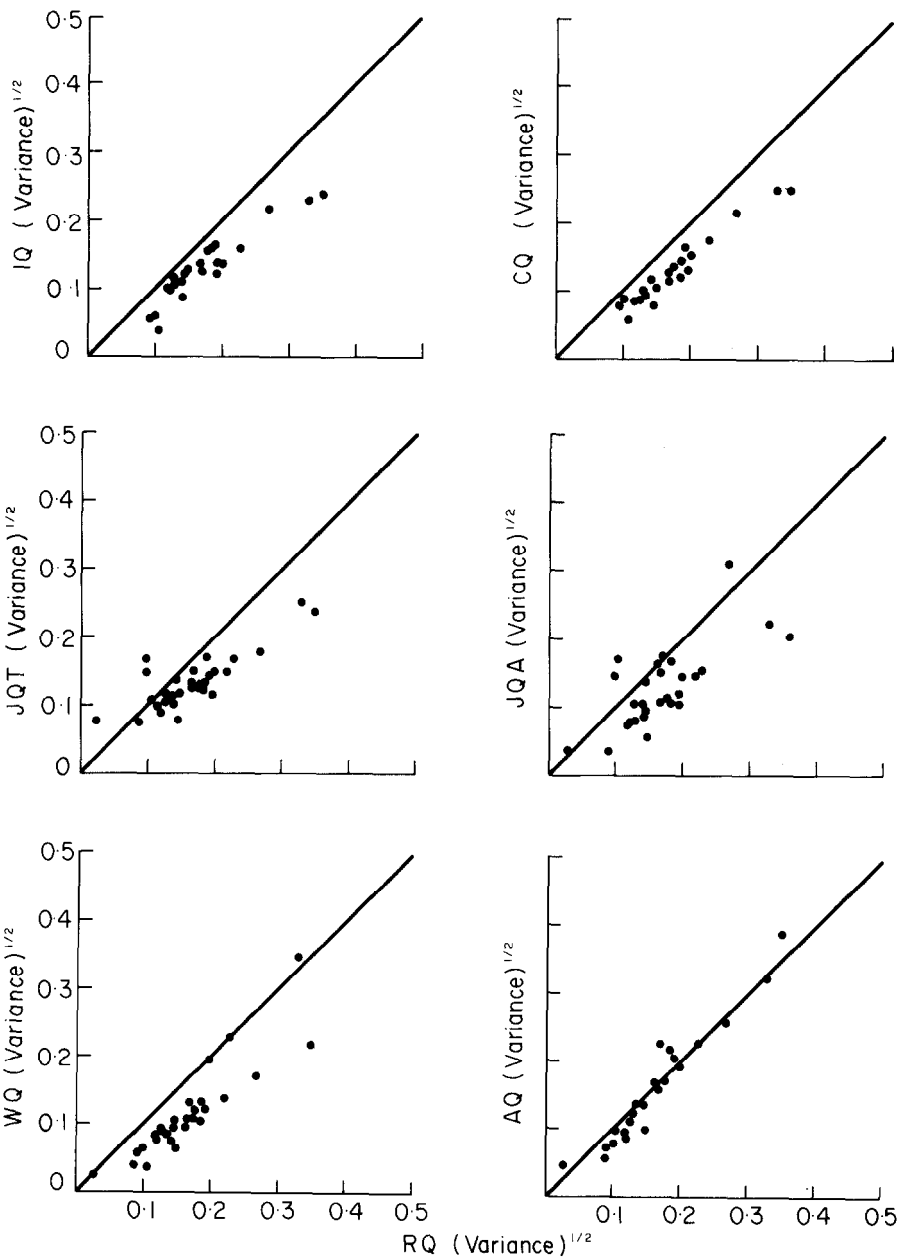

Fig. 10. Comparison of q-sensors in the form of σ_q in the middle spectrum band.

7.1.4. *q-sensors* (Reference RQ): σ_q

The individual values of σ_q in slice *B* are plotted in Figure 10, and relevant information given in Table VI.

TABLE VI

Comparison of σ_q in slice B for q sensors. The reference sensor RQ shares a mast with IQ and AQ (separation $\simeq$ 1 m). Sensors CQ, JQT, JQA, WQ are on a second mast (separation from RQ $\simeq$ 25 m)

Sensor	No. of runs	RMS difference δ (%)	Predicted RMS difference δ (%)	Mean difference Δ (%)
IQ	23	15.5	2	−25.9
AQ	23	14.6	2	−2.4
CQ	23	12.1	5.5	−27.0
JQT	30	24.6	5.5	−21.0
JQA	28	28.6	5.5	−24.4
WQ	31	16.9	5.5	−34.9

This represents the least satisfactory of all the comparisons and points to the state of the art for humidity sensors as compared with velocity and temperature sensors. Observed values of δ are much larger than those predicted suggesting instrumental instabilities.

Turning to Δ, it is seen that RQ and AQ are in substantial agreement, but very different from all other sensors which appear to agree with each other!

However, an inspection of the spectra indicated that the three psychrometers (CQ, JQT, JQA) are seriously in error due to the slow response of the wet bulb. Shaw and Tillman (1980) have developed a correction procedure for this based on an assumed similarity of the T_D and T_W spectra. Omitting the psychrometers, there still remains a significant calibration difference between the infra-red hygrometers (RQ and AQ) and the Lyman-α hygrometers (IQ and WQ). Further comments are delayed until discussion of the $w'q'$ covariance.

7.2. Comparison of covariances

Ideally, it would have been desirable to carry through an analysis similar to that for the variances, namely choose one of the reference arrays and compare other arrays with it for slice B of the spectrum. It soon became clear that the picture was extremely complex and that a somewhat different approach might be more helpful. The distortion of the flow field by supporting structures became a matter for serious consideration particularly for the central core experiment where a considerable concentration of sensors was experienced. Accordingly it was decided to use the eddy-fluxes measured in the micrometeorological support experiment as the reference fluxes. The reference covariances are not necessarily of higher quality than those measured in the central core experiment, but several advantages in choosing them include:

(i) mounting arrangements and/or exposure were generally superior in relation to possible flow distortion;

(ii) in general, continuity of operation was better;

(iii) the micrometeorological support experiment fluxes have already been assessed

for consistency with the measured profiles and with energy balance considerations (Garratt *et al.*, 1979).

A disadvantage of this method was the separation (125 m) between central core arrays and the reference instruments.

As a reference for the *uw* covariance, the average of at least three eddy fluxes from the two sonic anemometer systems and two Fluxatron systems operating in the micrometeorological support experiment were used. It will be remembered that these were corrected where necessary for sensor response and instrument tilt. Although an attractive possibility, the two drag plates were not used as references, since the data revealed an apparent trend with time during the experiment when compared with eddy flux measurements, presumably a reflection of the difficulties encountered in trying to match the drag plate surfaces with the surrounding site. Overall, however, the average of the drag plate measurements agreed with that of the eddy momentum fluxes.

For the *wT* covariance references, the average of three or more eddy fluxes of sensible heat from the two sonic systems and two Fluxatron systems of the micrometeorological support experiment were used. The lysimeter determinations of evaporation were used as reference for the *wq* covariances.

In the following, consideration has been given to corrections for

(i) Flow distortion,

(ii) Sensor response.

(iii) Lateral separation of sensors in a given array.

(iv) Calibration differences assessed in the σ comparison.

For the moment, the correction for flow distortion has been made by assuming the problem as equivalent to an error in vertical alignment (tilt) and the usual tilt corrections applied. It will be apparent from an earlier section where flow distortion is discussed more fully that this correction may be inadequate. In any case, where $\overline{w}$ and $\overline{u}$ were not retained in the instrument, this style of correction could not be made. Correction for

TABLE VII

Comparison of *uw* covariances with $\overline{u'w'}$ reference drawn from micrometeorological support experiment (see text). Bracketed figures indicate that no correction could be made for flow distortion

Sensor array	No. of runs	RMS difference with reference δ (%)	Mean difference (as measured) Δ (%)	Mean difference Δ (%) after successive correction for			
				Flow dist.	Sensor separation	Sensor response	Calibration difference
RW.RU	17	42	−4.7	(−5)	−5	−5	−11
WW.WU	14	45	−34	(−34)	−16	−16	−9
IW.IU	22	32	−49	(−49)	−8	3	13
JW.JU	23	28	−32	6	6	6	6
CW.CU	14	28	−13.7	33	33	33	24
AW.AU	18	36	−34.8	−30	−11	−1	6

Predicted RMS difference (23%).

sensor separation is based on the data of Table II. Correction for sensor response was applied in the case of the propellor anemometer *AW* and *IW*, using their known distance constants. Correction for calibration differences is based on the results of Tables III, IV, V, VI.

7.2.1. *Comparison of uw covariances*

The comparison of *uw* covariances as outlined above is listed in Table VII, and plotted in Figure 11.

Generally, the observed RMS differences are of the same order as those predicted. These relatively large values are largely a consequence of the small correlation coefficient between u and w at any one point, rather than the 125 m separation from the reference arrays, and illustrate the difficulty of drawing significant conclusions without a considerable amount of data.

The raw mean differences show wide variability, but considerable improvement appears after the application of the various corrections. The flow distortion correction appears to be quite significant for both the JW.JU and CW.CU covariances. However, it must be remembered that it has not been traditional practice to attempt a precise measurement of $\bar{w}$, and such corrections may be in error for this reason and also the possible inadequacy in this context of the normal tilt equations.

Systems using a vertical Gill propeller for w (IW.IU and AW.AU) benefit from the correction for sensor response. Sensor separation also appears to be a significant factor in a few cases.

It would appear from Table VII, that if proper care is taken in calibration, and if flow distortion and sensor separation are kept in mind, with correction for sensor response if necessary, then *uw* covariances could be obtained with a likely accuracy somewhat better than $\pm 15\%$ in the long term mean. Any individual 30 min Run would have an

TABLE VIII

Comparison of wT covariances with $\overline{w'T'}$ reference drawn from the micrometeorological support experiment (see text). Bracketed figures indicate that no correction could be made for flow distortion

Sensor array	No. of runs	RMS difference with reference δ (%)	Mean difference (as measured) Δ (%)	Mean difference Δ (%) after successive correction for			
				Flow dist.	Sensor separation	Sensor response	Calibration difference
RW.RT	25	41	5.3	(5)	5	5	0
WW.WT	12	17	−22.2	(−22)	−13	−13	4
IW.ITB	21	21	−24.2	(−24)	−20	−10	3
JW.JT	23	15	−9.1	−3	−3	−3	6
CW.CT	17	12	−15.1	−6	−6	−6	−3
AW.AT	22	13	−19.0	−20	−11	−1	8

Predicted RMS difference (14%).

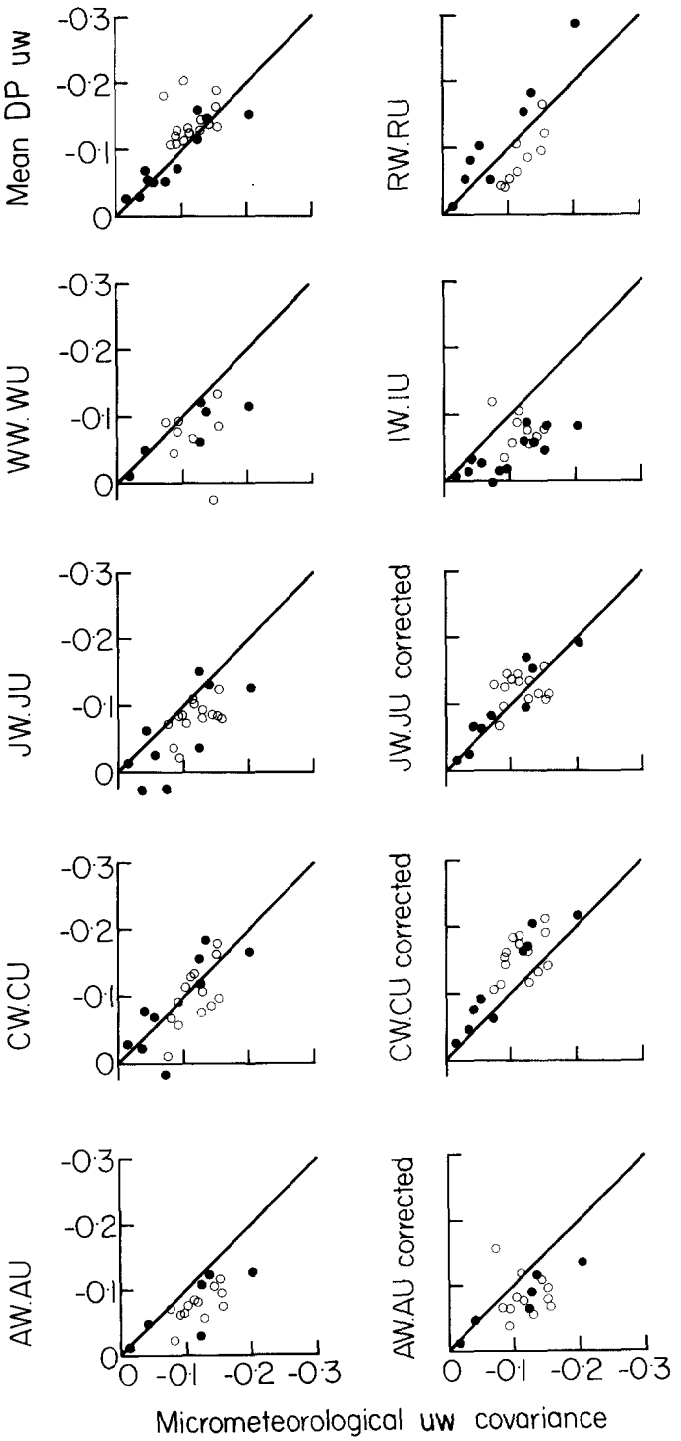

Fig. 11. Comparison of total *uw* covariance with *uw* reference.

uncertainty of ±23%. It seems probable that not all experiments reported in the past have been performed with this necessary degree of attention.

7.2.2. *Comparison of wT covariances*

Table VIII and Figure 12 present the comparison of wT covariances in the same manner.

It is well known that wT covariances usually show less variability than uw covariances, presumably a consequence of both less atmospheric variability (in steady radiation conditions) and less vulnerability to flow distortion problems. Such appears to be the case in Table VIII, as illustrated by the RMS differences, most of which are extremely close to the predicted values. No obvious explanation exists for the unusually high RMS difference reported by RW.RT.

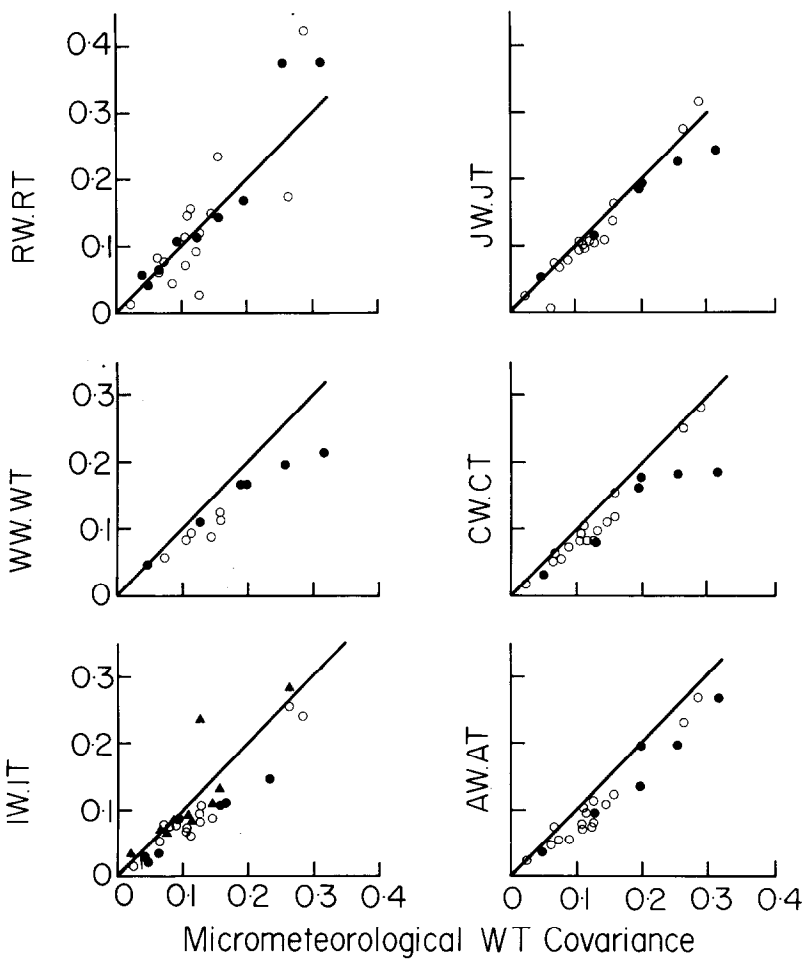

Fig. 12. Comparison of total wT covariances with wT reference.

Turning to the mean difference, it is again evident that the vertical Gill propeller system (IW.ITB and AW.AT) appear to derive some benefit from a correction for sensor response. JW.JT appear to be slightly improved by the flow distortion correction and WW.WT and AW.AT from the sensor separation correction.

With appropriate thought given in any experiment to the matters raised here, it seems likely that an accuracy of somewhat better than $\pm 10\%$ could be achieved in the long-term measurement of wT covariances, with an individual 30 min run having an uncertainty of about 14%.

7.2.3. *Comparison of wq Covariances*

Table IX and Figure 13 present the comparison of wq covariances.

All of the RMS differences reported were considerably greater than those predicted, probably pointing to the greater difficulty of humidity measurements. Mean differences show considerable variability. Two major problems emerge from these results. Firstly, the psychrometers showed a poor result, mainly due to the slow response time of the wet bulbs used. No attempt was made to correct for this because of the complex nature of a two-element system (T and T_W).

TABLE IX

Comparison of wq covariances with reference drawn from micrometeorological support experiment (see text). Bracketed figures indicate that no correction could be made for flow distortion

Sensor array	No. of runs	RMS difference with reference δ (%)	Mean difference (as measured) Δ (%)	Mean difference Δ (%) after successive correction for			
				Flow dist.	Sensor separation	Sensor response	Calibration difference
RW.RQ	22	46	2.7	(3)	3	3	3
WW.WQ	17	36	−35.6	(−36)	−36	−29	18
IW.IQ	13	20	−18.9	(−19)	−9	5	43
JW.JQT	22	50	−87.4	(−87)			
JW.JQA	20	39	−76.6	(−77)			
CW.CQ	14	27	−58.8	−52			
AW.AO	16	29	−18.4	−20	−11	−1	11

Predicted RMS difference (14%).

The difficulty is illustrated by a typical spectrum where the psychrometer systems report a negative spectral density at the higher frequencies. This is readily understood by reference to the approximate formula for a wet-bulb fluctuation q',

$$q' = \alpha T'_W - \beta T' ,$$

where for the conditions of this experiment $\alpha \simeq 0.96$, $\beta = 0.40$ with q in g kg^{-1} and T and T_W in deg K.

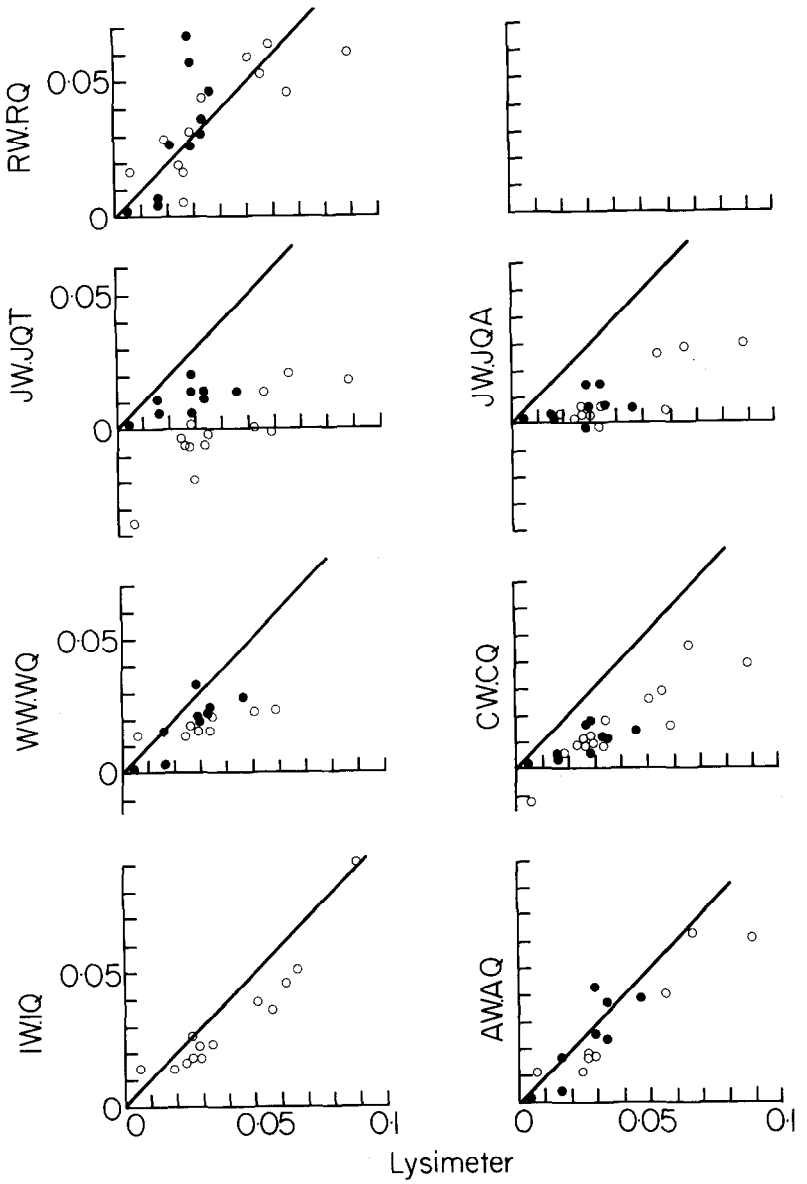

Fig. 13. Comparison of total wq covariances with wq reference.

Forming the covariance $\overline{w'q'}$, we have that

$$\overline{w'q'} = \alpha\overline{w'T'_w} - \beta\overline{w'T'} .$$

At the higher frequencies where the wet-bulb response has vanished, the apparent spectral density will be related to the sensible heat flux $\overline{w'T'}$, and of opposite sign, thus giving a negative version of the $\overline{w'T'}$ spectrum at these frequencies.

Further evidence is available through energy balance considerations, using net

radiation R, ground flux G, latent heat flux E and sensible heat flux H. L_W is the latent heat of vaporisation.

$$R - G = E + H$$
$$= \rho L_w \overline{w'q'} + \rho C_p \overline{w'T'}$$
$$= \rho L_W \alpha \overline{w'T'_W} \quad \text{since} \quad \beta \simeq C_p/L_W .$$

Table X presents a comparison of $\overline{w'T'_W}$ covariances with $R - G$, showing that a serious loss of the covariance $\overline{w'T'_W}$ and hence of $\overline{w'q'}$ will result. Because of this difficulty, no correction was attempted for the psychrometer instruments.

TABLE X

Comparison of $\overline{w'T'_W}$ covariances with $R - G$

Sensor array	Height (m)	n	$\rho L_W \alpha \overline{w'T'_W}$ (W m^{-2})	$R - T$ (W m^{-2})	Ratio
CW.CTW	4	17	162.5	264.5	0.61
CW.CTW	2.8	5	173.8	325.8	0.53
JW.JTW	4	15	172.1	299.1	0.58

Turning now to the other instruments, there is an obvious difficulty which has already been touched on in the comparison of $\overline{q'^2}$ variances.

The array RW.RQ requires no correction and agrees extremely well on the average with the reference value which in turn was also found to satisfy the energy balance. Thus there is considerable evidence supporting the RW.RQ result and hence the RQ instrument. For the other arrays, the agreement with the reference is 11% for AW.AQ, 18% for WW.WQ and 43% for IW.IQ. The previous σ_q comparison revealed some significant differences between RW and AQ on the one hand, and IW and WQ on the other, although the same degree of differences does not carry through to the $\overline{w'q'}$ covariances. If it were not for the IW.IQ result, one would probably claim an accuracy of the order of 10–20% for a long-term $\overline{w'q'}$ measurement made with due care. The uncertainty of the separation and sensor response corrections influences the confidence of the final comparison.

There appears to be a need to resolve this discrepancy in humidity calibration before further progress can be made in the confidence of a $\overline{w'q'}$ measurement. Certainly any worker would be well advised to make additional (R and G) measurements so that an energy balance check can be evaluated.

8. Final Conclusions of Sensor Comparisons

Variances and covariances measured by a number of instruments and instrument arrays have been compared to assess their field performance and calibration accuracy.

Meaningful comparisons have been made after due consideration has been given to the following factors:

(i) Instrumental response, which induces underestimates of the true variance and covariance.

(ii) Flow distortion induced by the instruments themselves and supporting structures. Tilt equations appear to represent only a first approximation to the required correction.

(iii) Spatial separation of the sensors used for covariance measurements, which generally induces an underestimate of the true covariance.

(iv) Statistical errors associated with single point measurements over a finite averaging time, and with the lateral separation of two sensors or sensor arrays being compared.

It should be emphasized that correction for both instrumental response and lateral separation of sensors used in covariance determinations are functions of height. In cases where significant corrections were required at the measurement height of 4 m, such instrument arrays would generally be used at heights of 10 m or more where corrections are greatly reduced.

For the u, w, T variances, the RMS differences were slightly greater than those estimates from statistical uncertainties alone, while those from q variances were much greater, pointing to greater instability of performance in the q sensors.

The mean difference (%) between sensors and reference for velocity and temperature was as great as 10% in some cases, presumably reflecting calibration differences. The mean difference (%) between humidity sensors revealed that infra-red sensors reported humidity fluctuations to be about 25% greater than did the Lyman-α sensors and the psychrometer sensors used in this experiment, the latter sensors, however, exhibiting some difficulties with slow-response wet bulbs. However, the latent heat fluxes based on the infra-red sensors agreed well with lysimeter values, which in turn were in good agreement with energy balance considerations, lending considerable weight to the confidence felt in the infra-red calibrations.

The RMS differences for wu and wT covariances were comparable with statistical estimates, but the corresponding differences for wq covariances were much higher than expected, presumably reflecting the greater difficulty of a humidity measurement.

The mean differences for wu and wT covariances, after successive approximate corrections had been applied, agreed generally to within $\pm$ 10%. For the wq covariances, final mean differences for the infra-red and Lyman-α devices lie within about 20% of each other. Raw values for the psychrometers used imply anomalously low covariances due to very slow wet bulbs. In this context it should be noted that Dyer (1961) provided a useful guide to the requirements of wet-bulbs in covariance measurements.

Overall the results emphasise the important effects of statistical error, and of flow distortion and sensor separation upon the covariance measurements. In the context of flow distortion, it is clear that constant attention must be devoted to sensor design and supporting structures, so that this distortion can be minimized. Where it is necessary to correct for flow distortion, it must be remembered that the conventional 'tilt' corrections may be somewhat inadequate, particularly for momentum measurements. Correc-

tion for lateral separation requires adequate knowledge of cross-correlation coefficients, and the need for this correction should also be minimised by good design.

9. Other Analyses of the Data

A secondary aim of the experiment was to provide information on flux-profile relationships, the von Karman constant, and the Kolmogarov constants. Analyses addressing these matters have been published separately (Francey and Garratt, 1981; Dyer and Bradley, 1982; Dyer and Hicks, 1982).

Acknowledgements

We are indebted to the management of Boonoke Station for permission to work on their property. Invaluable technical assistance was provided by many personnel from the CSIRO Divisions of Atmospheric Physics and Environmental Mechanics including in particular Jim Stevenson, Ian Bird, John Bryan, Guntis Grauze, David Murray, Graham Rutter, and Ian Helmond, and members of the respective Divisional workshops.

The foreign participants of ITCE 76 thank their Australian Colleagues from the CSIRO Division of Atmospheric Physics for the excellent organisation of the experiment.

References

Businger, J. A., Miyake, M., Dyer, A. J., and Bradley, E. F.: 1967, 'On the Direct Determination of the Turbulent Heat Flux Near the Ground', *J. Appl. Meteorol.* **6**, 1025–1032.

Businger, J. A., Miyake, M., Inove, E., Mitsuta, Y., and Hanafusa, T.: 1969, 'Sonic Anemometer Comparison and Measurements in the Atmospheric Surface Layer', *J. Meteorol. Soc. Japan* **47**, 1–12.

Businger, J. A., Wyngaard, J. C., Izumi, Y., and Bradley, E. F.: 1971, 'Flux-Profile Relationships in the Atmospheric Surface Layer', *J. Atmos. Sci.* **28**, 181–189.

Dyer, A. J.: 'Measurements of Evaporation and Heat Transfer in the Lower Atmosphere by an Automatic Eddy-Correlation Technique', *Quart. J. R. Meteorol. Soc.* **87**, 401–412.

Dyer, A. J.: 1981, 'Flow Distortion by Supporting Structures', *Boundary Layer Meteorol.* **20**, 243–251.

Dyer, A. J.: 1982, 'Reply', *Boundary-Layer Meteorol.* **22**, 267–268.

Dyer, A. J. and Bradley, E. F.: 1982, 'An Alternative Analysis of Flux-Gradient Relationships at the 1976 ITCE', *Boundary-Layer Meteorol.* **22**, 3–19.

Dyer, A. J., Garratt, J. R., and Francey, R. J.: 1981, 'The International Turbulence Comparison Experiment (Australia 1976). Central Core Data', CSIRO Div. of Atmos. Phys. Tech. Paper No. 38, 42 pp. (ISBN 0-643-00383-5).

Dyer, A. J. and Hicks, B. B.: 1982, 'Kolmogoroff Constants at the 1976 ITCE', *Boundary-Layer Meteorol.* **22**, 137–150.

Francey, R. J. and Garratt, J. R.: 1981, 'Interpretation of Flux-Profile Observations at ITCE (1976)', *J. Appl. Meteorol.* **20**, 603–618.

Garratt, J. R., Francey, R. J., McIlroy, I. C., Dyer, A. J., Helmond, I., Bradley, E. F., and Denmead, O. T.: 1979, 'The International Turbulence Comparison Experiment (Australia 1976) Micrometeorological Support Data', CSIRO Div. of Atmos. Phys. Tech. Paper No. 370, 23 pp. (ISBN 0-643-00352-50).

Hyson, P. and Hicks, B. B.: 1975, 'A Single-Beam Infrared Hygrometer for Evaporation Measurement', *J. Appl. Meteorol.* **14**, 301–307.

Kaimal, J. C., Wyngaard, J. C., Izuma, Y., and Cote, O. R.: 1972, 'Spectral Characteristics of Surface Layer Turbulence', *Quart. J. R. Meteorol.* **98**, 563–589.

Koprov, B. M. and Sokolov, D. Yu.: 1973, 'Spatial Correlation Functions of Velocity and Temperature Components in the Surface Layer of the Atmosphere', *Izv. Atmos. and Oceanic Phys.* **9**, 178–182.

Lumley, J. L. and Panofsky, H. A.: 1964, 'The Structure of Atmospheric Turbulence', John Wiley and Sons, New York, 239 pp.

Lynch, R. A. and Bradley, E. F.: 1974, 'Shearing Stress Meter', *J. Appl. Meteorol.* **13**, 588–591.

Miyake, M., Stewart, R. W., Burling, R. W., Tsvang, L. R., Koprov, B. M., and Kuznetov, O. M.: 1971, 'A Comparison of Acoustic Instruments in the Measure of Atmospheric Turbulent Flow over Water', *Boundary-Layer Meteorol.* **2**, 228–245.

Pasquill, F.: 1962, 'Atmospheric Diffusion', D. Van Nortrand Co. Ltd., London, pp. 429.

Shaw, W. J. and Tillman, J. E.: 1980, 'The Effects of and Correction for Different Wet Bulb and Dry-Bulb Response in Thermocouple Psychrometry'.

Tsvang, L. R., Koprov, B. M., Zubrovski, S. L., Dyer, A. J., Hicks, B. B., Miyake, M., Stewart, R. W., and McDonald, J. W.: 1973, 'A Comparison of Turbulence Measurements by Different Instruments. Tsimlyansk Field Experiment 1970', *Boundary-Layer Meteorol.* **3**, 499–521.

Wyngaard, J. C.: 1973, in Duane A. Haugen (ed.), 'Workshop on Micrometeorology', American Met. Society, Boston, pp. 101–148.

Wyngaard, J. C.: 1982, 'Comments on Flow Distortion by Supporting Structures', *Boundary-Layer Meteorol.* **22**, 263–265.